Published OnlineFirst January 20, 2021; DOI: 10.1158/0008-5472.CAN-20-1959



# The *BRCA1* Pseudogene Negatively Regulates Antitumor Responses through Inhibition of Innate Immune Defense Mechanisms

Yoo Jane Han[1], Jing Zhang[1], Jung-Hyun Lee[2,3], Jennifer M. Mason[4], Olga Karginova[1], Toshio F. Yoshimatsu[1], Qinyu Hao[5], Ian Hurley[1], Laia Paré Brunet[6,7], Aleix Prat[6,7], Kannanganattu V. Prasanth[5], Michaela U. Gack[2,3], and Olufunmilayo I. Olopade[1]

## ABSTRACT

Innate immune defense mechanisms play a pivotal role in antitumor responses. Recent evidence suggests that antiviral innate immunity is regulated not only by exogenous non–self-RNA but also by host-derived pseudogene RNAs. A growing body of evidence also indicates a biological role for pseudogenes as gene expression regulators or immune modulators. Here, we report an important role for *BRCA1P1*, the pseudogene of the *BRCA1* tumor-suppressor gene, in regulating innate immune defense mechanisms in breast cancer cells. *BRCA1P1* expresses a long-noncoding RNA (lncRNA) in breast cancer cells through divergent transcription. Expression of lncRNA-*BRCA1P1* is increased in breast tumors compared with normal breast tissues. Depletion of *BRCA1P1* induces an antiviral defense-like program, including the expression of antiviral genes in breast cancer cells. Furthermore, *BRCA1P1*-deficient cancer cells mimic virus-infected cells by stimulating cytokines and inducing cell apoptosis. Accordingly, depletion of *BRCA1P1* increases host innate immune responses and restricts virus replication. In converse, overexpression of *BRCA1P1* reduces cytokine expression in breast cancer cells. Mechanistically, lncRNA-*BRCA1P1* is localized in the nucleus, binds to the NF-κB subunit RelA, and negatively regulates antiviral gene expression. Finally, in a xenograft mouse model of breast cancer, depletion of *BRCA1P1* stimulates cytokine expression and local immunity, and suppresses tumor growth. Our results suggest an important role for *BRCA1P1* in innate immune defense mechanisms and antitumor responses. This mechanism of antiviral immunity regulated by a host-derived pseudogene RNA may guide the development of novel therapies targeting immune responses in breast cancer.

**Significance:** This study identifies a novel mechanism of innate immunity driven by a host pseudogene RNA that inhibits innate immune defense mechanisms and antitumor responses through regulation of antiviral gene expression.

## Introduction

Innate antiviral immunity is a significant mechanism in cancer (1). It mediates intrinsic antitumor responses through several mechanisms, which include triggering of apoptosis of cancer cells, stimulating spontaneous DNA damage, and increasing antitumor efficacy of radiotherapy and chemotherapy. Both cancer cells and virus-infected cells threaten the host by expressing neo-antigens and by evading control mechanisms of host immune surveillance. Cancer cells can actually mimic a viral infection process by activating RNA-sensing pattern recognition receptors (PRR) and by stimulating cytokine production and activating cytotoxic immune cells, the latter killing infected cells via externally induced cell lysis and apoptosis. RIG-I and MDA5 of the RIG-I–like receptor (RLR) family are important PRRs involved in the detection of RNA viruses (2, 3). RLRs initiate host antiviral responses that induce type I IFNs and other cytokines, leading to the transcription of hundreds of IFN-stimulated genes (ISG; ref. 4). Activation of RLRs by dsRNA ligands not only triggers host immune responses but can also directly induce apoptosis of cancer cells, in an IFN-dependent or independent manner (5). Consequently, cancer cells are highly susceptible to RLR-induced cell death via intrinsic and extrinsic apoptosis and immune activation, indicating that the signaling pathway driven by RLRs is a promising molecular pathway to target in cancer immunotherapy.

Interestingly, recent evidence suggests that antiviral innate immunity is regulated not only by exogenous non–self-RNA but also by host-derived pseudogene RNAs. Pseudogenes have been considered nonfunctional artifacts of evolutionary processes due to degenerative features such as the accumulation of disruptive mutations or their lack of regulatory elements (6, 7). However, a growing body of evidence indicates biological roles for pseudogenes as gene expression regulators or immune modulators. 5S ribosomal RNA pseudogene transcripts, in particular *RNA5SP141*, were shown to bind to RIG-I and induce the expression of antiviral cytokines during infection with herpes simplex virus type 1 or the related herpes virus Epstein–Barr virus (8). Lethe, a pseudogene long-noncoding RNA (lncRNA), is selectively induced by proinflammatory cytokines or glucocorticoid receptor agonists, and serves as a functional regulator of inflammatory signaling (9). These data suggest that pseudogenes may play a role in regulating antiviral defense and inflammatory signaling pathways.

[1]Department of Medicine, Center for Clinical Cancer Genetics and Global Health, University of Chicago, Chicago, Illinois. [2]Department of Microbiology, University of Chicago, Chicago, Illinois. [3]Florida Research and Innovation Center, Cleveland Clinic, Florida, Port Saint Lucie, Florida. [4]Department of Genetics and Biochemistry, Clemson University, Clemson, South Carolina. [5]Department of Cell and Developmental Biology, Cancer Center at Illinois, University of Illinois at Urbana-Champaign, Urbana, Illinois. [6]Translational Genomics and Targeted Therapies in Solid Tumors, IDIBAPS, Barcelona, Spain. [7]Department of Medicine, University of Barcelona, Barcelona, Spain.

**Note:** Supplementary data for this article are available at Cancer Research Online (http://cancerres.aacrjournals.org/).

**Corresponding Authors:** Yoo Jane Han, University of Chicago, Medicine, 900 East 57th Street, Chicago, IL, 60637. E-mail: yjhan@medicine.bsd.uchicago.edu; and Olufunmilayo I. Olopade, folopade@medicine.bsd.uchicago.edu

Cancer Res 2021;81:1540–51

**doi:** 10.1158/0008-5472.CAN-20-1959

Published OnlineFirst January 20, 2021; DOI: 10.1158/0008-5472.CAN-20-1959



The chromosome 17q21 region containing *BRCA1* has a partially duplicated pseudogene, *BRCA1P1* (Gene ID: 394269, HUGO ID: 28470), which contains only three of the 24 exons of *BRCA1* (10–12). It also includes an insertion of the acidic ribosomal phosphoprotein P1 pseudogene (*RPLP1P4*) in exon 1a, displaying unique features of a chimeric pseudogene derived from the two parent genes, *BRCA1* and *RPLP1*. The presence of *BRCA1P1* on the same chromosome close to *BRCA1* appears to create a hotspot for homologous recombination (13), leading to genomic rearrangements between *BRCA1P1* and *BRCA1* in families with a high risk of breast and ovarian cancers. *BRCA1* deficiency is frequently observed in breast, ovarian, and other cancers (14, 15). Although the roles of BRCA1 in regulating homologous recombination and DNA damage repair have been extensively studied (16), the biological relevance of *BRCA1P1* pseudogene in breast cancer has not been elucidated.

In this study, we discovered an important role for *BRCA1P1* in regulating antiviral program-like responses in breast cancer cells. In contrast with BRCA1's involvement in homologous recombination repair, *BRCA1P1*-depleted cancer cells resemble virus-infected cells, and express high amounts of ISGs and cytokines, which ultimately make them more susceptible to cell death. In a breast cancer xenograft mouse model, *BRCA1P1* depletion suppresses tumor growth and stimulates proinflammatory cytokines and local immunity. To our knowledge, this is the first study that demonstrates an important role of *BRCA1P1* pseudogene in antitumor responses through regulation of antiviral innate immunity and tumor growth.

## Materials and Methods

### Primary breast cancer tissue samples and RNA extraction

We obtained written informed consent from the patients for anonymous use of banked tumor tissues for research. The studies were conducted in accordance with recognized ethical guidelines of the Declaration of Helsinki, and were approved by an institutional review board at the University of Chicago Medical Center. Methods for case selection, tumor RNA extraction, microarray and RNA sequencing were described previously (17). In brief, we selected female patient cases with invasive ductal carcinoma from our Breast Program Biospecimen Bank. Patients who had received neoadjuvant chemotherapy were excluded, as we were interested in pretreatment gene expression. Areas of malignant tissue were isolated from frozen tissues and homogenized by the Tissue Lyzer LT (Qiagen). RNA was extracted using the Qiagen AllPrep DNA/RNA/Protein Mini Kit protocol (Qiagen). The integrity of RNAs was validated using a 2100 Bioanalyzer (Agilent) at the University of Chicago Genomics Facility. RNAs with a minimum RNA integrity number of 8 were used for cDNA synthesis and qRT-PCR experiments. Molecular subtypes of the breast tumors were determined by mRNA expression of the PAM50 intrinsic classifier as previously described (17).

### Animal study and handling

All animals were humanely handled and monitored for health conditions according to the Institutional Animal Care and Use Committee–approved protocols. Eight-week-old female *Foxn1nu/nu* (Harlan) mice were anesthetized via inhalation with 2% vaporized isoflurane and were unilaterally injected with $4 \times 10^6$ MDA-MB-231 wild-type (WT) or *BRCA1P1*-knockout (KO) cells (100 μL, 50% Matrigel, 8–9 animals per model) into the fourth inguinal mammary gland at the base of the nipple. Tumor measurements were performed weekly using calipers to calculate tumor volume using the formula: 1/2 (Length × Width$^2$). The assessment was blind to the animal model and was performed by the same person throughout the study. Animal weight was monitored twice weekly. Spleens were collected from animals in each model at the end of the study for downstream experiments.

### Cell culture

Primary human mammary epithelial cells (HMEC) were purchased from Lonza. Breast cancer cells were obtained from the ATCC. Cells were authenticated for species and unique DNA profile using short tandem repeat (STR) analysis by the provider (ATCC). Cells were cultured in media recommended by the ATCC, and tested negative for *Mycoplasma* contamination using the MycoAlert Kit (Lonza).

### Cell transfection and drug-sensitivity assay

Cells were seeded at $3–5 \times 10^5$ cells/well on 6-well plate and transfected with 20–50 nmol/L of BRCA1P1-ASO (LNA GapmeRs, Exiqon) or 2 μg of poly(I:C) (InvivoGen) using DharmaFECT 1 or 4 (Dharmacon), or Lipofectamine 3000 transfection reagent (Invitrogen). One day after transfection, cells were transferred to 96-well cell culture plates at $1–1.5 \times 10^4$ cells/well. Chemotherapy drugs (5 μmol/L doxorubicin or 4 μmol/L camptothecin; Sigma-Aldrich) were added to cells one day after transfer, and incubated for 24 hours. The Caspase-Glo 3/7 Assay (Promega) was used to screen apoptotic cells by measuring luminescent signals using a Synergy H1 Plate Reader (BioTek).

### CRISPR-Cas9 knockout and activation

Guide RNAs (gRNA) were designed using the chopchop tools (http://chopchop.cbu.uib.no/), IDT Alt-R CRISPR-Cas9 guide RNA (https://www.idtdna.com/site/order/designtool/index/CRISPR_CUSTOM) or sgRNA designer (https://portals.broadinstitute.org/gpp/public/analysis-tools/sgrna-design) and synthesized by Integrated DNA Technologies. Two pairs of gRNAs were designed to delete 1,147 bp (gRNAs 1 and 4) or 1,469 bp (gRNAs 2 and 3) of the *BRCA1P1* sequence. For CRISPR activation (CRISPRa), three gRNAs were designed to target the *BRCA1P1* promoter. DNA sequences of gRNAs will be provided upon request. The KO experiment was performed as previously described in the literature (18). Briefly, gRNAs were cloned into pSpCas9 (BB)-2A-GFP (Addgene #48138) and pSpCas9 (BB)-2A-Puro (Addgene #62988) using the BbsI restriction enzyme site. For CRISPRa, we used SP-dCas9-VPR (Addgene #63798). MDA-MB-231 cells were cotransfected with gRNAs using Lipofectamine 3000 (Invitrogen) and incubated for two days. For the isolation of *BRCA1P1*-KO clones, cells were treated with puromycin (1 μg/mL) for one week, diluted to one cell per 100 μL media and plated into each well of a 96-well plate. Single colony cells were expanded and subjected to PCR validation and DNA sequencing.

### Total RNA extraction and microarray analysis

T47D and MDA-MB-231 cells were transfected with control or BRCA1P1-ASOs, incubated for 24 hours, and processed for RNA purification. MDA-MB-231 cells with *BRCA1P1*-KO or WT genotype were also subjected to RNA purification. Total RNAs were isolated with the RNeasy kit (Qiagen) following the protocol provided by the manufacturer. To avoid any possibility of DNA contamination, total RNAs were treated with RNase-free DNase I (Qiagen). Quality control was performed with the Agilent 4200 TapeStation system (Agilent). RNAs with RNA integrity numbers greater than eight were selected and subjected to the Illumina Human HT12 microarray platform. The microarray data were analyzed by significance analysis of microarrays (SAM) between control or BRCA1P1-ASO–treated cells or between *BRCA1P1*-KO and WT cells. The significant gene expression in ASO-treated cells in microarray experiments was identified and

Published OnlineFirst January 20, 2021; DOI: 10.1158/0008-5472.CAN-20-1959



subjected to DAVID functional annotation bioinformatics microarray analysis. The microarray datasets are available through GEO (GSE112572 and GSE112573).

### Viral infection assays

Sendai virus (SeV, Cantell strain) was purchased from Charles River Laboratories. Cells were infected with SeV at 5 HAU/mL and lysed at 8, 16, and 24 hours after infection for quantitative real-time PCR (qRT-PCR). VSV-eGFP was kindly provided by Sean Whelan (Harvard). Cells were infected with VSV-eGFP at MOI of 0.005 and analyzed for eGFP expression using flow cytometry (LSR Fortessa flow cytometer, BD Biosciences) after 8, 16, and 24 hours later. For flow cytometry, cells were harvested and then pelleted by centrifugation at 300 × *g* for 5 minutes. Cells were washed with PBS and fixed with 4% (v/v) paraformaldehyde in PBS at room temperature for 30 minutes, followed by washing cells twice with PBS. The main cell population was gated in the FCS/SSC blot and then analyzed in the FITC channel. Positive cells were above the cutoff value, which is set to 98% of measurable events of the negative control.

### IncuCyte live-cell proliferation and apoptosis analysis

Cells were plated at 5,000 cells/well in 96-well plates and allowed to adhere for 24 hours. IncuCyte Caspase-3/7 Green reagent was added to the media at a 1:1,000 dilution (Essen Bioscience No. 4440). Images of live cells were acquired using a 10× objective every 2 hours (four images/well) with the IncuCyte S3 live-cell analysis system. Data were analyzed using IncuCyte analysis software. Cell density was quantified as a measure of cell proliferation. Apoptosis was quantified as the total integrated intensity of green fluorescent signal from cells with activated caspase-3/7 (apoptotic cells) normalized to cell density calculated from phase-contrast images. The experiment was performed twice with 7–10 technical replicates.

### Statistical analysis

Each experiment was repeated at least three times and the mean ± standard deviation (SD) or mean ± standard error (SE) is shown with *t* test (unpaired, two-tailed) values. Statistical significance was set at *, $P < 0.05$; **, $P < 0.01$; ***, $P < 0.001$; and ****, $P < 0.0001$. We performed one-way ANOVA to compare the expression level across the breast tumor subtype groups. Statistical analysis was carried out using Microsoft Excel and GraphPad Prism 6.0 (GraphPad Software, Inc.). Plots were generated using GraphPad Prism 6.0.

### Availability of data and materials

The microarray datasets are available through GEO (GSE112572 and GSE112573). There are no restrictions on availability of data. The data that support the findings of this study are available from the corresponding author upon request.

More detailed Materials and Methods are included in Supplementary Information. The oligonucleotides and antibodies used in the experiments are listed in Supplementary Tables S1 and S2, respectively.

## Results

### The genomic structure and degenerative mutations in the *BRCA1P1* pseudogene

The chromosome 17q21 region comprising the *BRCA1P1* pseudogene shows parallel elements of genomic structure, as *BRCA1* is located head-to-head with *NBR2*, and *BRCA1P1* is located head-to-head with *NBR1* (**Fig. 1A**). Cross-species comparative analysis among chicken, mouse, and human revealed that the *BRCA1P1* pseudogene is present only in the human genome. A comparison of DNA sequences between *BRCA1* and *BRCA1P1* showed that the pseudogene contains only three exons (exons 1a, 1b, and 2), with three major insertions that include a 343 bp insertion of the *RPLP1* pseudogene (*RPLP1P4*) in exon 1a (10) and two ALU element insertions in exon 1b and intron 1b of *BRCA1P1* (**Fig. 1B**). Notably, exon 2 contains a point mutation that alters the translation initiation codon (ATG) of *BRCA1P1* to ATA. On the basis of the degenerative mutations occurring in the pseudogene (insertions and a start codon mutation), we predicted no protein coding potential for *BRCA1P1* transcripts.

### A bidirectional promoter shapes the transcription of the *BRCA1P1* pseudogene

To determine whether the *BRCA1P1* pseudogene is expressed through the bidirectional promoter between *BRCA1P1* and *NBR1*, we cloned the 1,243 bp region of the *BRCA1P1* promoter into a luciferase reporter gene construct and assessed the promoter activity in T47D cells (**Fig. 1C**). Sequence homology analysis between the *BRCA1* and *BRCA1P1* promoters showed that 85.7% of the promoter regions were identical. The *BRCA1P1* promoter exhibits a 9.6 ± 1.0-fold increase in luciferase activity compared with a $pGL_3B$ empty vector. Using this active promoter, the *BRCA1P1* pseudogene is transcribed from exon 1a to exon 1b (including introns) with a resulting RNA of at least 1,629 nucleotides [details in Supplementary Methods (characterization of *BRCA1P1* transcripts) and Supplementary Fig. S1].

### Expression of *BRCA1P1* is increased in breast cancer cells and breast tumors

We surveyed *BRCA1P1* expression in breast cell lines and breast tumors of different molecular subtypes and genetic backgrounds (**Fig. 1D–F**). Three pairs of primers were designed to quantify the pseudogene transcripts from exon 1a, exon 1b, and intron 1a to exon 1b (unspliced form), respectively (Supplementary Fig. S2A). Because a spliced form of the *BRCA1P1* transcript was previously reported in HeLa cells (12), we first compared the expression between the spliced and unspliced (intron 1a to exon 1b) forms. This analysis showed that the majority of the *BRCA1P1* transcripts (98%) are not spliced in T47D and MDA-MB-231 cells (Supplementary Fig. S2B).

Using primers detecting unspliced transcripts of *BRCA1P1*, we assessed *BRCA1P1* expression in several breast cancer cell lines. A comparison of *BRCA1P1* expression between nonmalignant and malignant breast cells showed an average 2.8-fold increased expression in breast cancer cell lines compared with primary mammary epithelial cells (HMEC; **Fig. 1D**). Expression of *BRCA1P1* in MDA-MB-231 and T47D cells was 2.86 ± 0.96 and 3.63 ± 1.10-fold higher than that in HMEC, respectively. Next, we examined *BRCA1P1* expression in 36 frozen primary breast tissues of different molecular subtypes (**Fig. 1E** and **F**). Molecular subtypes of the breast tumors were determined by mRNA expression of the PAM50 intrinsic classifier (19). Expression of *BRCA1P1* increased by 2.1-fold in breast tumors compared with normal breast tissues, with no subtype-specific pattern of expression. Together, these data indicate that breast cancer cells and tumors exhibit elevated *BRCA1P1* expression compared with normal breast epithelial cells or normal breast tissues.

### Depletion of *BRCA1P1* induces antiviral immune gene expression

To determine the biological role of the pseudogene in breast cancer, we inhibited expression of *BRCA1P1* in breast cancer cells using two different approaches. First, antisense oligonucleotides (ASO, LNA GapmeRs) were custom designed to target exon 1a of *BRCA1P1*. The

Published OnlineFirst January 20, 2021; DOI: 10.1158/0008-5472.CAN-20-1959



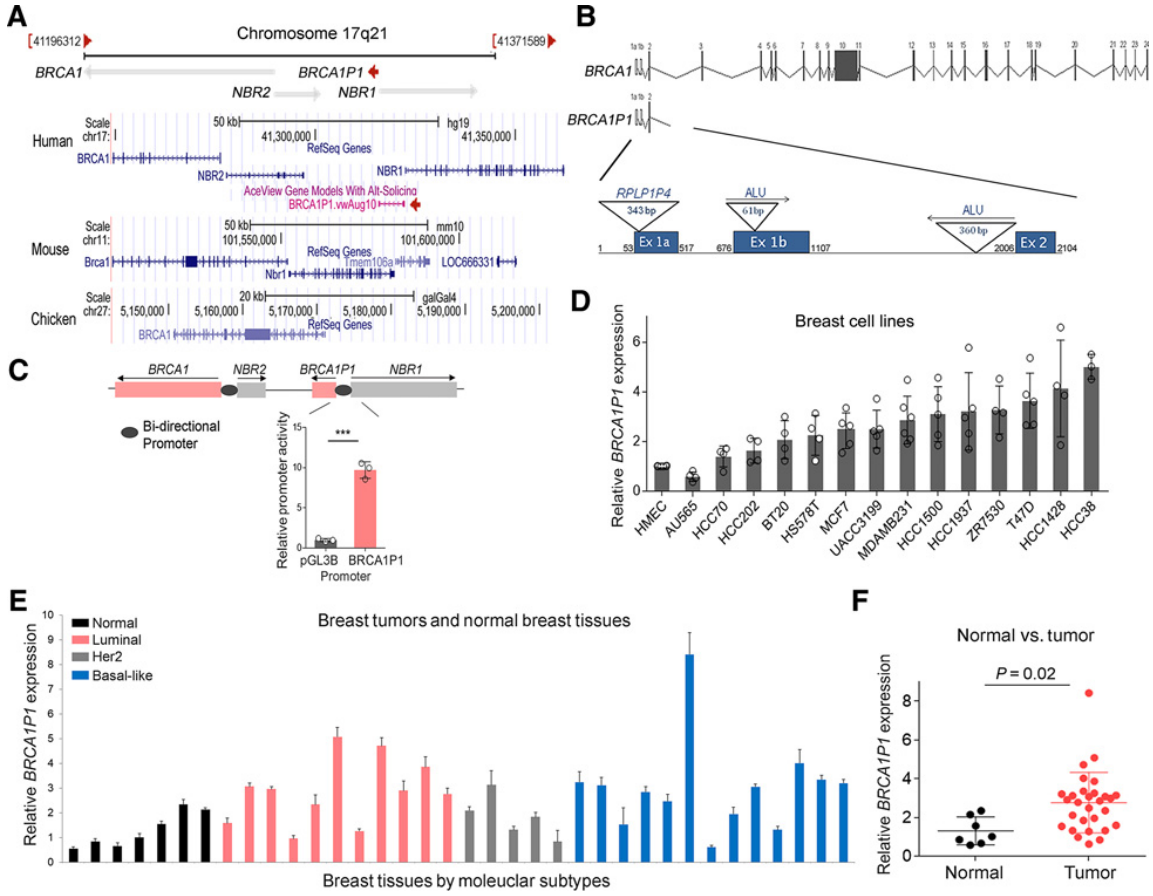


**Figure 1.**

Genomic structure, promoter activity and expression of the *BRCA1P1* pseudogene in breast cells and tissues. **A,** Schematic representation of the genomic organization of chromosome 17q21 (GRCh37/hg19), as shown in the NCBI genomic context (top). The UCSC genome browser view of chromosome 17q21 (NCBI36/hg18) shows the presence of the *NBR2* gene and *BRCA1P1* pseudogene in humans but not in mice or chickens (bottom). **B,** Depicted are the exonic and intronic structures of *BRCA1P1. BRCA1P1* retains only three exons (exon 1a, 1b, and 2) out of 25 exons of the parent *BRCA1* gene. The numbers represent nucleotide positions starting with the transcription start site. Insertions of a pseudogene of acidic ribosomal phosphoprotein P1 *(RPLP1P4)* and two ALU elements are presented. **C,** Bidirectional promoters are located between *BRCA1* and *NBR2*, and between *BRCA1P1* and *NBR1*. Promoter activity was assessed in T47D cells using dual luciferase activity assays, which showed greater *BRCA1P1* promoter activity compared with a pGL3B empty vector. Error bars represent the SD of three biological replicates. ***, $P < 0.001$. **D,** qRT-PCR was performed on HMECs and 14 human breast cancer cell lines using the primers detecting the unspliced transcripts of *BRCA1P1*. Results were normalized to *RNA18S* (18S ribosomal RNAs) and fold induction is shown relative to HMEC cells. Data represent mean and SD of four to six independent experiments. **E** and **F,** *BRCA1P1* expression was analyzed in 36 frozen primary breast tissues (relative to expression in normal breast tissue) and grouped by molecular subtypes: normal breast tissues ($n = 7$), luminal ($n = 11$), Her2-positive ($n = 5$), basal-like breast tumors ($n = 13$; **E**). Expression of *BRCA1P1* showed a significant increase in breast tumors ($n = 29$) compared with normal breast tissues ($n = 7$; $P = 0.022$; **F**).

efficiency of knockdown by ASO was validated at the RNA expression level using qRT-PCR (Supplementary Fig. S2C). The expression of *BRCA1P1* was significantly dampened by BRCA1P1-specific ASO, with no silencing effect on the expression of the parent genes (*BRCA1* and *RPLP1*) or adjacent genes (*NBR1*) in T47D and MDA-MB-231 cells. Second, we deleted the *BRCA1P1* pseudogene from the genome of MDA-MB-231 cells using CRISPR-Cas9 genome-editing tools (Supplementary Fig. S3A). Cotransfection of two guide RNAs (gRNA1 and 4) resulted in a partial deletion (1,147 bp) of the *BRCA1P1* pseudogene (Supplementary Fig. S3B), with no inhibitory effects on the parent gene (*BRCA1*) expression (Supplementary Fig. S3C).

To identify genes and pathways influenced by *BRCA1P1* loss or depletion, we performed genome-wide gene expression profiling (**Fig. 2A**). This analysis identified 3,981 upregulated genes in BRCA1P1-ASO–treated groups compared with control-ASO groups both in T47D and MDA-MB-231 cells, as well as 723 upregulated genes in *BRCA1P1*-KO cells compared with the WT cells. One hundred and thirteen genes were upregulated in both *BRCA1P1*-KO and knockdown (ASO-treated) cells. Gene ontology enrichment analysis of the 113 overlapping genes revealed the antiviral defense response as one of the most upregulated pathways.

Validation of microarray data by qRT-PCR confirmed increased expression of antiviral ISGs [*IFIT3*, MDA5 (*IFIH1*), RIG-I (*DDX58*), *HERC6*, and *APOBEC3B*] in two clones of *BRCA1P1*-KO compared with WT control cells (**Fig. 2B**). Protein expression of IFIT3, MDA5, and RIG-I was also significantly increased in the KO clones compared

Published OnlineFirst January 20, 2021; DOI: 10.1158/0008-5472.CAN-20-1959



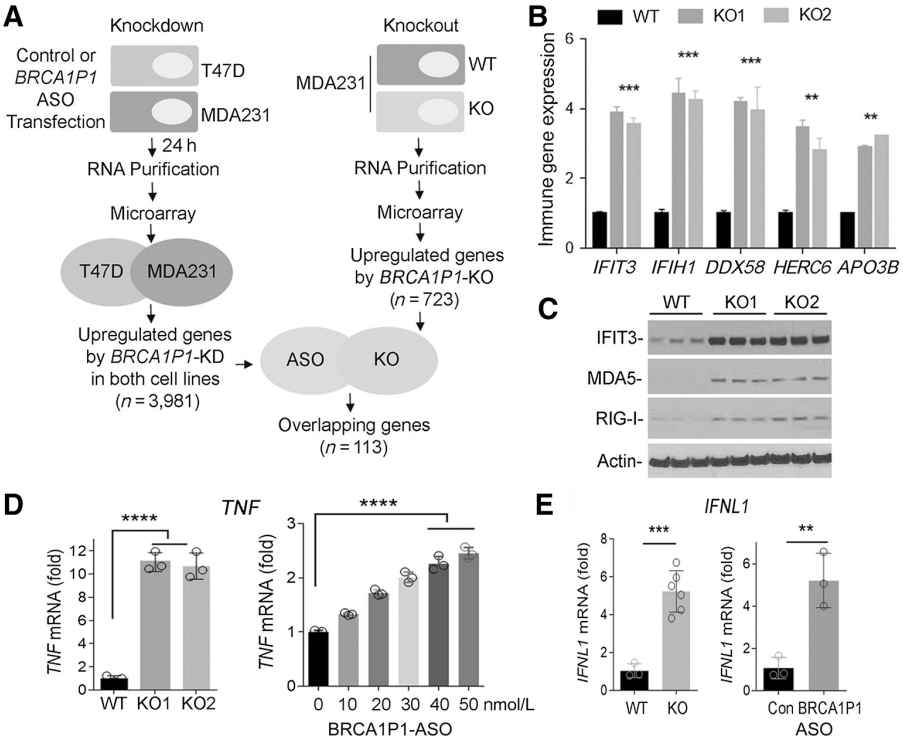


**Figure 2.**

Upregulation of antiviral genes and cytokines in *BRCA1P1*-depleted cells. **A,** Experimental schema of gene expression microarray analysis in *BRCA1P1* knockdown (KD) and knockout (KO) cells. T47D and MDA-MB-231 cells treated with ASOs (left). MDA-MB-231 cells with *BRCA1P1*-wild type (WT) or KO genotype (right) were also subjected to RNA purification and microarray analysis. The analysis identified 3,981 and 723 upregulated genes in BRCA1P1-ASO–treated and KO cells compared with controls, respectively, with 113 genes overlapping between KD and KO cells. **B,** qRT-PCR analysis of antiviral genes [*IFIT3, IFIH1* (MDA5), *DDX58* (RIG-I), *HERC6*, and *APOBEC3B*] in *BRCA1P1*-KO clones compared with the WT. Results were normalized to *RNA18S* and fold induction is shown relative to control WT cells. **C,** Western blot analysis showed increased expression of IFIT3, MDA5, and RIG-I in *BRCA1P1*-KO clones compared with the WT. β-Actin was used as an endogenous control. **D** and **E,** Expression of *TNF* or *IFNL1* mRNA was analyzed using qRT-PCR in *BRCA1P1*-KO cells (left) or BRCA1P1-ASO–treated cells (right). Increasing concentration of BRCA1P1-ASO gradually increases expression *TNF* mRNA in T47D cells. All results were normalized to *RNA18S* and fold induction is shown relative to WT control cells (left) or control-ASO–treated cells (right). Data represent mean and SD of $n = 3$ to $n = 6$ biological replicates and are representative of at least two independent experiments. **, $P < 0.01$; ***, $P < 0.001$; ****, $P < 0.0001$.

with control cells (**Fig. 2C**). The data suggested that *BRCA1P1* deficiency triggered an innate immune defense program characterized by transcriptional upregulation of many antiviral genes.

### Loss of *BRCA1P1* stimulates cytokine expression

Because the replication and spread of viral pathogens are restricted by innate immune mechanisms and most prominently cytokine signaling, we next examined whether loss of *BRCA1P1* stimulated cytokine expression. We used qRT-PCR to analyze cytokine expression because basal cytokine expression levels in breast cancer cells are extremely low, and thus often undetectable by microarrays. We found a dramatic increase in *TNF* expression in *BRCA1P1*-depleted cells compared with control cells (**Fig. 2D**). Expression of *TNF* was 10.7 ± 1.1- and 11.0 ± 0.8-fold greater in two *BRCA1P1*-KO clones, respectively, compared with the WT cells (left, **Fig. 2D**). *TNF* expression also gradually increased in T47D cells treated with increasing concentrations of BRCA1P1-ASOs (right, **Fig. 2D**). Of note, we did not observe any expression of type I IFNs (*IFNA1* and *IFNB1*) in MDA-MB-231 cells using qRT-PCR (Supplementary Fig. S4A and S4B). Copy-number alteration data in the Cancer Cell Line Encyclopedia revealed a frequent deletion of type I IFN genes in cancer cell lines (Supplementary Fig. S4D). In accord, MDA-MB-231 cells carry homozygous (deep) deletions of 17 subtypes of IFNα and IFNβ genes. In contrast, the expression of type III IFN (*IFNL1*) was markedly increased in MDA-MB-231 cells, compared with nonmalignant HMEC cells (Supplementary Fig. S4C). Furthermore, loss of *BRCA1P1* led to a significant increase in *IFNL1* expression in MDA-MB-231 cells compared with the WT cells (left, **Fig. 2E**). Knockdown of *BRCA1P1* using ASO also increased *IFNL1* expression, compared with control-ASO–treated cells (right, **Fig. 2E**). Collectively, our data indicate that loss of *BRCA1P1* stimulates the expression of cytokines (TNFα and IFNλ) and a range of antiviral ISGs.

### Antiviral-like program induced by *BRCA1P1*-depletion

We next determined the effect of *BRCA1P1* loss on virus-induced antiviral gene expression and virus replication in MDA-MB-231 cells (**Fig. 3A–C**). SeV (*Paramyxoviridae*) and eGFP-expressing vesicular stomatitis virus (VSV-eGFP, *Rhabdoviridae*) are well

Published OnlineFirst January 20, 2021; DOI: 10.1158/0008-5472.CAN-20-1959



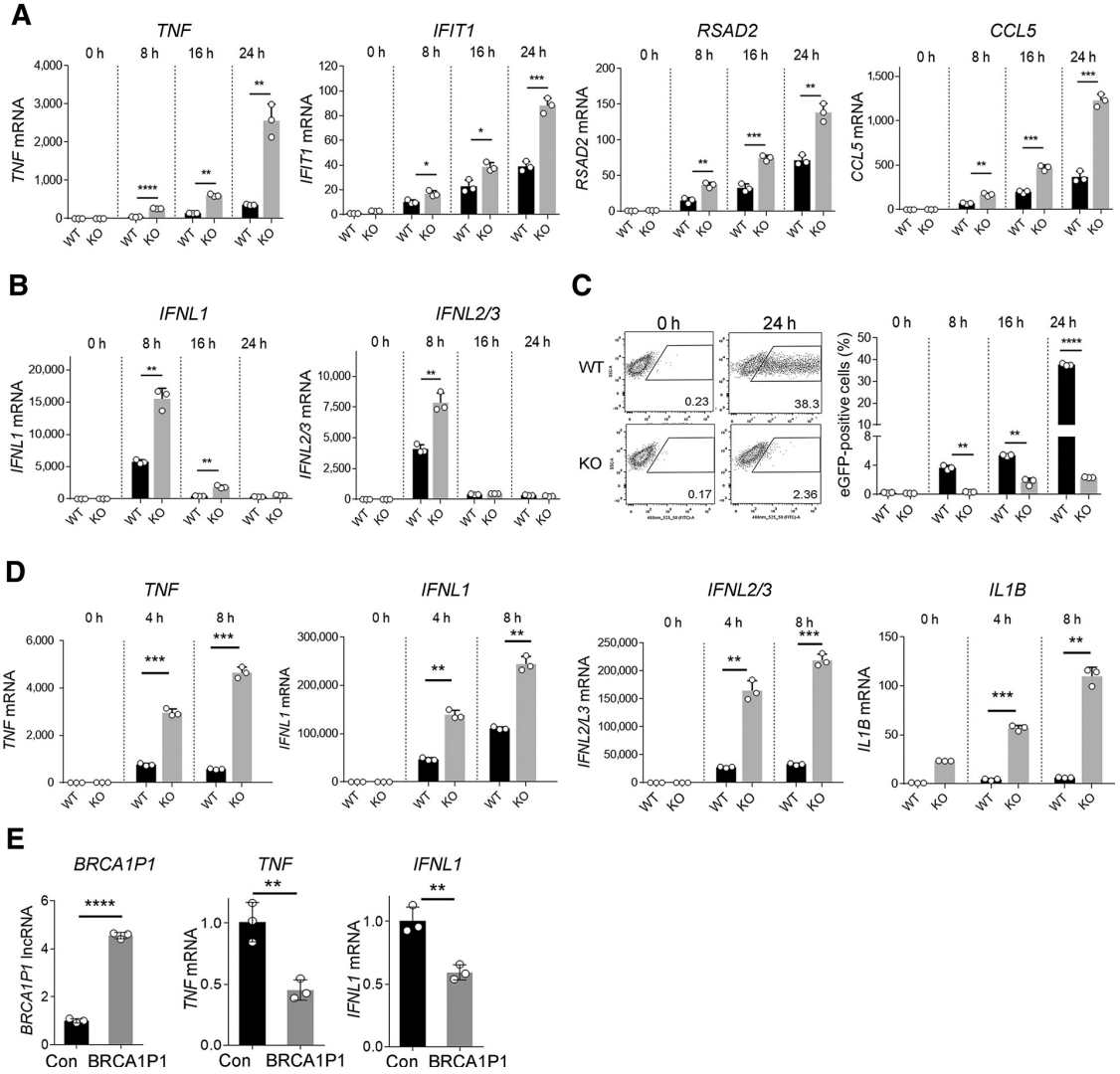


**Figure 3.**

Innate immune responses after viral infection, poly(I:C) transfection, or *BRCA1P1* overexpression. **A** and **B,** qRT-PCR analysis of *TNF, IFIT1, RSAD2, CCL5, IFNL1,* and *IFNL2/L3* mRNA in *BRCA1P1*-KO and WT cells that were infected with Sendai virus (SeV, 5 HAU/mL) for the indicated times. Results were normalized to *GAPDH* and fold induction is shown relative to mock-infected control cells. Data represent mean and SD of $n = 3$ biological replicates and are representative of at least two independent experiments. *, $P < 0.05$; **, $P < 0.01$; ***, $P < 0.001$; ****, $P < 0.0001$. **C,** MDA-MB-231 WT and *BRCA1P1*-KO cells were infected with eGFP-expressing vesicular stomatitis virus (VSV-eGFP) at multiplicity of infection of 0.005. The percentage of eGFP-positive cells was determined by flow cytometry for the indicated times. Error bars, SD of three biological replicates. **, $P < 0.01$; ****, $P < 0.0001$. **D,** qRT-PCR analysis of *TNF, IFNL1, IFNL2/3,* and *IL1B* mRNA in *BRCA1P1*-KO and WT cells transfected with poly(I:C) at 4 and 8 hours after transfection (**, $P < 0.01$; ***, $P < 0.001$ vs. poly I:C treated WT). **E,** The effect of BRCA1P1 overexpression on cytokine expression. *BRCA1P1* expression was stimulated in MDA-MB-231 cells using the CRISPR activation system (left), which led to a decrease in *TNF* and *IFNL1* expression (middle and left). Fold induction is shown relative to control cells (no sgRNA treatment). Data represent mean and SD of $n = 3$ biological replicates and are representative of at least two independent experiments. **, $P < 0.01$; ****, $P < 0.0001$.

known to trigger innate immune responses via activation of the RLR signaling pathway. The expression of cytokine/chemokine (*TNF* and *CCL5*) and ISGs (*IFIT1* and *RSAD2*) during SeV infection was significantly higher in *BRCA1P1*-KO cells than in infected WT cells (**Fig. 3A**). In particular, the expression of *TNF* was greatly increased in *BRCA1P1*-KO cells compared with the WT cells at 24 hours after SeV infection (a 2,568.1 ± 431-fold vs. 361.7 ± 16.1-fold increase). The expression of *IFNL1* and *IFNL2/L3* was also greater in the KO cells at 8 hours after infection (a 14,527 ± 1,520-fold vs. 5,754 ± 320-fold increase; **Fig. 3B**). In accord, cells depleted of *BRCA1P1* suppressed the replication of VSV-eGFP more effectively than did the WT cells [2.36 vs. 38.3 eGFP-positive cells (relative units)] (**Fig. 3C**). Collectively, these findings indicated that loss of *BRCA1P1* triggered a cytokine-mediated antiviral program.

Published OnlineFirst January 20, 2021; DOI: 10.1158/0008-5472.CAN-20-1959



### Poly(I:C)-driven antiviral signaling in breast cancer cells

Previous reports showed that poly(I:C), a synthetic analogue of double-stranded RNAs, binds to cytosolic RIG-I and MDA5 receptors (20, 21) and induces innate immune signaling that leads to the cytosol-to-nuclear translocation of several key transcription factors [e.g., NF-κB, IFN-regulatory factors (IRF), and AP-1; ref. 22]. To determine whether *BRCA1P1* regulates cytokine expression through activation of transcription factors, we first examined poly(I:C)-driven nuclear translocation of NF-κB in breast cancer cells (Supplementary Fig. S5A). In MDA-MB-231 cells, as in fibroblast cells, nuclear localization of the NF-κB subunit RelA increased upon poly(I:C) transfection, starting from 4 to 8 hours after transfection. Next, as MDA-MB-231 cells express type III IFNs (Supplementary Fig. S4C), we examined nuclear transport of IRF1, which plays a major role in type III IFN induction. We observed an increase in IRF1 nuclear localization at 4 to 8 hours after poly(I:C) transfection. A rapid increase in *TNF* and *IFNL* expressions was also observed starting at 4 to 8 hours after treatment, followed by increases in expression for ISGs (*IFIT3, IFIH1*, and *DDX58*), ILs (*IL8, IL6, IL1A*, and *IL1B*), and the transcription factors (*IRF1, STAT1*, and *STAT2*; Supplementary Fig. S5B and S5C).

We then compared poly(I:C)-induced gene expression between *BRCA1P1*-WT and KO cells (**Fig. 3D**). This analysis showed significant increases in the expression of *TNF* (a 4,660 ± 136-fold vs. 575 ± 15-fold increase), *IFNL1* (a 244,948 ± 8,898-fold vs. 111,222 ± 1,845-fold increase) and *IFNL2/3* (a 219,251 ± 6,429-fold vs. 33,140 ± 1,105-fold increase) in *BRCA1P1*-KO cells compared with the WT cells at 8 hours after treatment. It is of note that we were able to measure gene expression only up to 8 hours after treatment because poly(I:C)-transfected *BRCA1P1*-KO cells were severely apoptotic and not able to survive for longer times. The expression of ILs (*IL1A, IL1B*, and *IL6*) and antiviral genes [*IFIH1* (MDA5) and *STAT1*] was also significantly higher in *BRCA1P1*-KO cells than in WT cells (Supplementary Fig. S6). These data suggested that depletion of *BRCA1P1* sensitized breast cancer cells to apoptosis by stimulating expression of cytokines.

We also investigated the effect of *BRCA1P1* overexpression on *TNF* and *IFNL* expression in breast cancer cells (**Fig. 3E**). To stimulate *BRCA1P1* expression using its own promoter and to express *BRCA1P1*-lncRNA in the proper subcellular location (nucleus), we used the CRISPR activation system (CRISPRa), which led to a 4.5-fold increase in *BRCA1P1* expression in MDA-MB-231 cells (left). Overexpression of *BRCA1P1* significantly decreased expression of *TNF* and *IFNL1* compared with the control vector-transfected cells (middle and right). The overexpression data together with the depletion data indicate that *BRCA1P1* regulates *TNF* and *IFNL* expression in breast cancer cells.

### Association of *BRCA1P1*-lncRNA with the NF-κB subunit RelA

To understand the mechanism whereby *BRCA1P1* regulates cytokine expression, we first determined the subcellular localization of *BRCA1P1*-lncRNA using two different methods (**Fig. 4A**). Fractionation of cellular compartments showed a strong enrichment of *BRCA1P1*-lncRNA in the nuclei of T47D, CAMA-1 and HCC-1937. Single-molecule RNA-FISH (smRNA-FISH) revealed that the majority of *BRCA1P1* signals in cancer cells were restricted to the nucleus, whereas most *GAPDH* signals were detected in the cytoplasm (**Fig. 4A**). Together, these data showed nuclear localization of *BRCA1P1* transcripts.

We thus tested whether *BRCA1P1* interacts with transcription factors important for innate immune signaling in the nucleus of MDA-MB-231 cells. Specifically, we focused on NF-κB, IRF1 and STAT-1 because these transcription factors are known to regulate expression of *TNF, IFNL* and/or ISGs in response to viral infection or dsRNA stimulation. RNA immunoprecipitation data revealed an association of *BRCA1P1*-lncRNA with the NF-κB subunit RelA, but not with IRF1 or STAT-1 (**Fig. 4B**). *RNA18S5* (18S rRNA), which served as a negative control, exhibited no interaction with any of them. These data suggested a specific interaction of *BRCA1P1*-lncRNA with RelA in the nucleus.

### Inhibition of RelA activity by *BRCA1P1*

To determine whether the interaction of *BRCA1P1*-lncRNA with RelA influences the enrichment of RelA at the target promoters, we conducted chromatin immunoprecipitation of RelA proteins on the promoters of *TNF, IFNL1*, and *IFIH1* genes (**Fig. 4C**). We observed greater abundance of the RelA transcription factor at the promoters in *BRCA1P1*-KO cells compared with WT cells. Inversely, overexpression of *BRCA1P1* decreased RelA enrichment at the promoters of *TNF, IFNL1*, and *IFIH1* (**Fig. 4D**).

We also performed an electrophoretic mobility shift assay to determine whether *BRCA1P1*-lncRNA inhibits the association of RelA with the target promoters (**Fig. 4E**). As expected, we observed a strong association of recombinant RelA proteins (p65) with an NF-κB cis–acting regulatory element at the TNF promoter, indicated by the retardation in electrophoretic mobility of the probe on PAGE (lane 2, **Fig. 4E**). In contrast, the strength of this interaction decreased with increasing amounts (1 to 10 fmols) of *BRCA1P1*-lncRNA in a dose-dependent manner (lanes 3–5, **Fig. 4E**). The specificity of RelA's interaction with the motif was confirmed by further retardation in mobility (super-shift) resulting from interaction with anti-RelA antibodies (lane 6). These data further strengthen the deduction that *BRCA1P1*-lncRNA interferes with RelA's binding to target promoters.

Next, we generated truncated mutants of *BRCA1P1*-lncRNA and conducted RNA pull-down assays with recombinant RelA proteins (**Fig. 4F** and **G**). Whereas there was a strong association of *BRCA1P1*-lncRNA (1–1107 nt) with RelA (lane 1, **Fig. 4G**), deletion of exon 1a in *BRCA1P1*-lncRNA strongly decreased its interaction with RelA (lanes 3 and 4). In contrast, deletion of exon 1b and intron 1a had only a minor effect on the interaction (lane 2). These results suggest that exon 1a is important for the interaction of *BRCA1P1*-lncRNA with RelA. An RNA structure prediction showed that exon 1a forms a long stretch of small hairpin loops, which might play a role in its interaction with RelA (Supplementary Fig. S7A), although this remains to be determined. Collectively, these data showed that *BRCA1P1*-lncRNA physically interacts with RelA in part through exon 1a, inhibits NF-κB binding to promoters, and negatively regulates target gene expression.

Finally, we determined whether depletion of NF-κB abrogates *BRCA1P1* loss-driven *TNF* expression (**Fig. 4H**). Depletion of *BRCA1P1* increased *TNF* expression (a 57.8 ± 13.9-fold increase) in control siRNA-treated cells, which was reduced to a 23.2 ± 8.9-fold increase in RelA siRNA-treated cells. The expression of *IFNL1* was also reduced by RelA silencing (a 43.9 ± 9.2 *vs.*62.6 ± 6.2-fold increase). Collectively, the data reinforce the observation that *BRCA1P1* regulates expression of *TNF* and *IFNL1* partly through NF-κB.

### Depletion of *BRCA1P1* increases apoptosis of breast cancer cells

A radical defense mechanism to restrict the spread of a viral infection is apoptosis of the infected cell. We found that *BRCA1P1*-deficient cells are apoptotic, with an increased frequency of caspase-3/7–positive cells in *BRCA1P1*-KO and BRCA1P1-ASO–treated cells compared with the WT cells and control-ASO–treated cells,

Published OnlineFirst January 20, 2021; DOI: 10.1158/0008-5472.CAN-20-1959



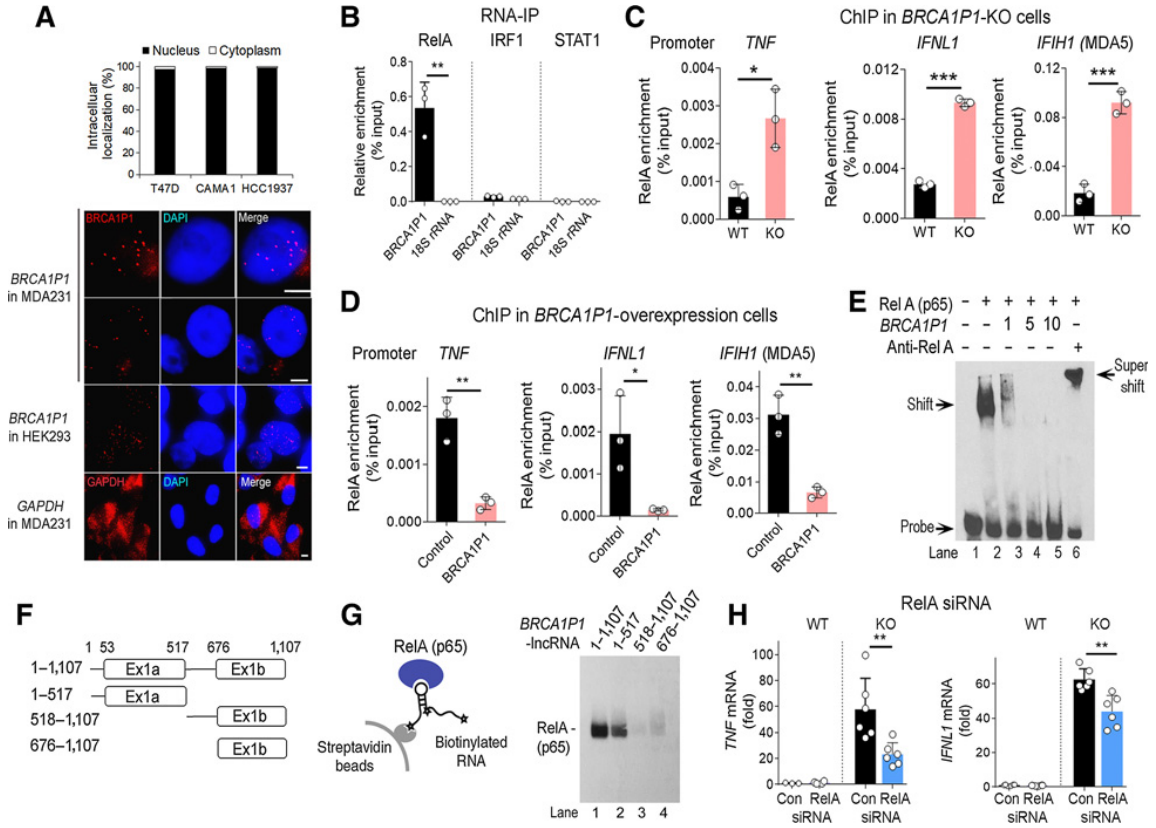


**Figure 4.**

*BRCA1P1*-lncRNA interacts with nuclear RelA and regulates its binding to promoters. **A,** The intracellular expression level of *BRCA1P1* was quantified by qRT-PCR using cytoplasmic or nuclear fractions of breast cancer cells (T47D, CAMA1, and HCC-1937; top). Representative images show single-molecule RNA FISH results performed in MDA-MB-231 and HEK293 cells using 26 oligonucleotide probes tiling *BRCA1P1* (bottom). Fluorescent signals from *BRCA1P1*-lncRNA (red) were observed in nuclei, whereas *GAPDH* mRNA signals (control) were found in cytoplasm. **B,** RNA immunoprecipitation (RNA-IP) was conducted in MDA-MB-231 cells using antibodies against transcription factors (RelA, IRF1, and STAT1). Enrichment of *BRCA1P1*lncRNA is shown relative to input RNA (% input). 18S rRNA, *JPX* lncRNA, and *BRCA1* mRNA were used as negative controls. Data represent mean and SD of $n = 3$ to $n = 4$ biological replicates and are representative of at least two independent experiments. **, $P < 0.01$; ****, $P < 0.0001$ vs. negative controls. **C** and **D,** Chromatin immunoprecipitation (ChIP) was performed in *BRCA1P1*-KO (**C**) or *BRCA1P1*-overexpression cells (**D**) using antibodies against RelA. Enrichment of RelA at the promoters of *TNF, IFNL1*, and *IFIH1* is shown relative to input DNA (% input). Error bars, SD of three biological replicates. *, $P < 0.05$; **, $P < 0.01$; ***, $P < 0.001$. **E,** Electrophoretic mobility shift assays were performed using biotin-labeled oligonucleotides containing the cis-acting regulatory NF-κB element of the TNF promoter. Recombinant RelA proteins (200 ng), *BRCA1P1*-lncRNA (1, 5, or 10 fmols), or anti-RelA antibodies (200 ng) were incubated with oligonucleotides (2 fmols) and subjected to 6% PAGE. The arrow indicates the mobility of free oligonucleotides (probe), oligonucleotides associated with RelA (shift), or oligonucleotides associated both with RelA and anti-RelA antibodies (super-shift). **F,** Depicted are the truncated mutants of *BRCA1P1* with exon 1a to exon 1b (1–1107nt), exon 1a only (1–517nt), intron 1a to exon 1b (518–1107nt), or exon 1b only (676–1107nt). **G,** RNA pull-down assays were conducted using the truncated mutants of *BRCA1P1*-lncRNA, which were transcribed *in vitro*, labeled with biotin at their 3′ ends, bound to streptavidin beads, and incubated with recombinant RelA (p65) proteins (left). Western blot analysis followed by RNA pull-down assays showed RelA proteins associated with the truncated mutants of *BRCA1P1* (right). **H,** qRT-PCR analysis of *TNF* and *IFNL1* mRNA in *BRCA1P1*-KO and WT cells that were transfected with RelA siRNA for 24 hours. Results were normalized to *RNA18S* and fold induction is shown relative to control siRNA-treated cells. Data represent mean and SD of $n = 6$ biological replicates and are representative of at least two independent experiments. **, $P < 0.01$.

respectively (left, **Fig. 5A** and **B**). The increases in apoptosis appeared to restrict the proliferation of these cells, demonstrated by clear decreases in cell density of *BRCA1P1*-KO cells and BRCA1P1-ASO–treated cells, compared with the respective control cells (right, **Fig. 5A** and **B**). To determine whether the observed phenotypes (apoptosis and proliferation) are driven by *BRCA1P1* specifically, we re-expressed *BRCA1P1* in BRCA1P1-ASO–treated cells using CRISPRa (**Fig. 5B**). Re-expression of *BRCA1P1* reduced apoptosis and restored proliferation of BRCA1P1-ASO–treated cells to the same levels as those observed in control-ASO–treated cells, demonstrating the specificity of *BRCA1P1*-driven regulation of apoptosis and proliferation in breast cancer cells. Interestingly, we did not observe any change in cell proliferation or apoptosis driven by *BRCA1P1* depletion in HMEC cells (**Fig. 5C**), indicating that *BRCA1P1* regulates apoptosis in cancer cells but not in normal breast cells.

### TNFα induced apoptosis in *BRCA1P1*-depleted cells

We next tested whether cytokines induced apoptosis in *BRCA1P1*-KO cells. This is based on our data showing increased cytokine expression in *BRCA1P1*-KO cells (**Fig. 2D** and **E**), as well

Published OnlineFirst January 20, 2021; DOI: 10.1158/0008-5472.CAN-20-1959



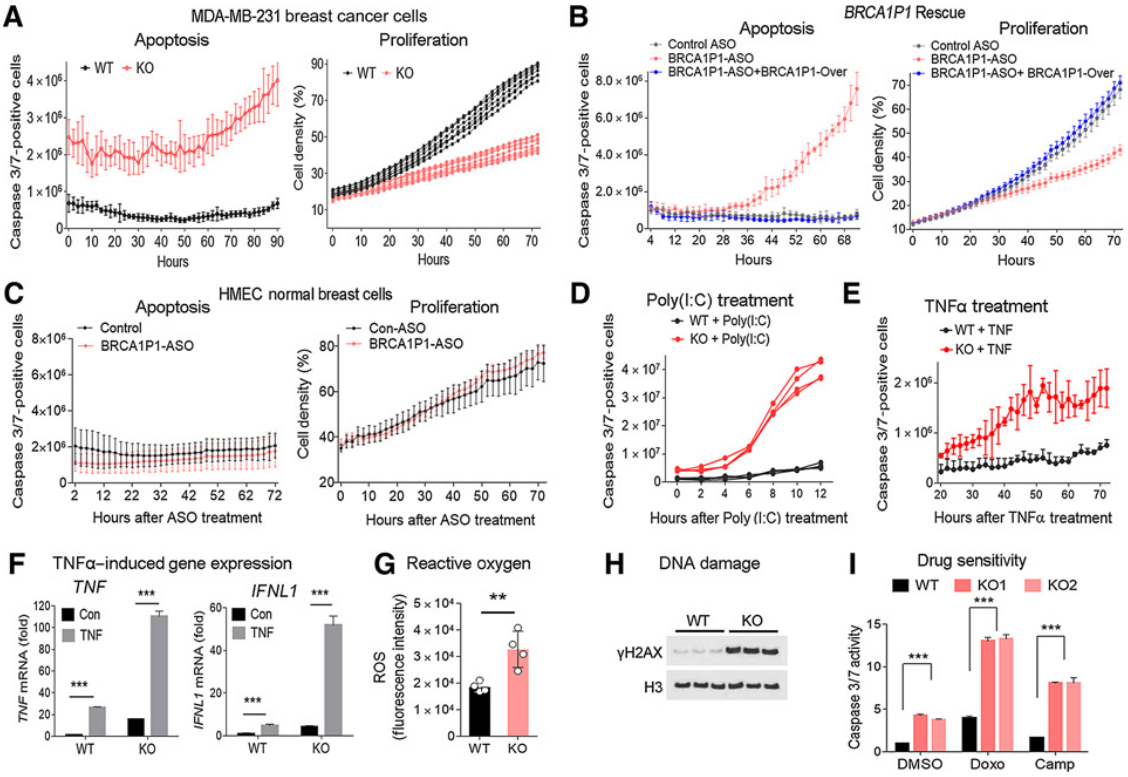


**Figure 5.**

Increased apoptosis and drug sensitivity of *BRCA1P1*-depleted cells. **A,** Apoptosis and proliferation of *BRCA1P1*-WT and KO cells were analyzed using the IncuCyte Live-Cell Imaging System. Apoptosis was quantified using green fluorescent signals from caspase-3/7–positive apoptotic cells normalized to cell density (left), whereas cell density values were derived from phase-contrast images of cells to evaluate cell proliferation (right). Data represent mean and SD of $n = 4$ to 10 biological replicates and are representative of at least two independent experiments. **B,** MDA-MB-231 cells were treated with control-ASO, BRCA1P1-ASO, or BRCA1P1-ASO, followed by CRISPR activation of *BRCA1P1* (BRCA1P1-Over). Apoptosis and proliferation of the cells were analyzed using the IncuCyte system. **C,** HMEC cells were treated with control-ASO or BRCA1P1-ASO and subjected to IncuCyte imaging. **D** and **E,** *BRCA1P1*-WT and KO cells were treated with poly(I:C) or TNFα (25–30 ng/mL) for indicated times. Caspase-3/7–positive apoptotic cells were assessed using the IncuCyte Caspase-3/7 Green assay. **F,** Expression of *TNF* or *IFNL1* mRNA was analyzed using qRT-PCR in *BRCA1P1*-KO and WT cells treated with TNFα for 40 hours. All results were normalized to *RNA18S* and fold induction is shown relative to WT control cells (untreated). Data represent the mean and SD of $n = 3$ biological replicates and are representative of at least two independent experiments. ***, $P < 0.001$. **G,** ROS were measured in *BRCA1P1*-KO and WT cells using 2′,7′-dichlorofluorescin diacetate (DCFDA). The *y*-axis represents the geometric mean of DCFDA fluorescence intensity. Data represent the mean and SD of $n = 4$ biological replicates and are representative of at least two independent experiments. **, $P < 0.01$. **H,** Western blot analysis of H2AX phosphorylation (γH2AX) in *BRCA1P1*-WT and KO cells. Histone3 (H3) was used as a loading control for nuclear proteins. **I,** Apoptosis was measured in response to doxorubicin (Doxo) and camptothecin (Camp) in *BRCA1P1*-KO clones using caspase-3/7 activity assays. Data represent the means of $n = 4$ biological replicates and are representative of at least two independent experiments (***, $P <$ 0.001 vs. WT cells or control-ASO treated).

as previous literature reporting the pivotal role of TNFα in the regulation of apoptosis (23, 24). We treated *BRCA1P1*-KO and WT cells with poly(I:C) or TNFα, and examined the effects on apoptosis and cytokine expression. Treatment of cells with poly(I:C) induced higher *TNF* expression (**Fig. 3D**) and more severe apoptosis in *BRCA1P1*-KO cells than it did in control cells (**Fig. 5D**). Treatment with TNFα clearly increased apoptosis of *BRCA1P1*-KO cells with an average 3.9-fold increase compared with WT cells at 52 hours after treatment (**Fig. 5E**). The increase in apoptosis was accompanied by strongly elevated expression of *TNF* and *IFNL1* in *BRCA1P1*-KO cells (**Fig. 5F**).

Because previous reports showed that TNFα induces apoptosis through reactive oxygen species (ROS) and DNA damage (23–27), we determined whether apoptosis driven by *BRCA1P1* depletion is partly due to accumulation of ROS and DNA damage. In line with this, we observed significant increases in ROS and H2AX phosphorylation (γH2AX), a well-known DNA damage marker, in *BRCA1P1*-KO cells compared with the WT cells (**Fig. 5G** and **H**). Our data indicate that TNFα induces apoptosis of *BRCA1P1*-KO cells, partly through accumulation of ROS and DNA damage. Furthermore, we observed that *BRCA1P1*-depleted cells were more sensitive to genotoxic drugs, with increased apoptosis after doxorubicin and camptothecin treatment in *BRCA1P1*-KO cells (**Fig. 5I**), compared with the WT cells. Together, our data suggest that *BRCA1P1* depletion increases apoptosis and sensitizes breast cancer cells to genotoxic drug treatments.

### Depletion of *BRCA1P1* inhibits tumor growth *in vivo*

To determine the physiological role of *BRCA1P1* in regulating tumor growth and antitumor immunity *in vivo*, we injected MDA-MB-231 cells of either the *BRCA1P1* WT or KO genotype into

Published OnlineFirst January 20, 2021; DOI: 10.1158/0008-5472.CAN-20-1959



the mammary glands of female athymic nude mice [(Crl:NU(NCr)-Foxn1nu]. In control mice that were injected with *BRCA1P1*-WT cells ($n = 8$), tumor volumes increased over time, up to a volume of 494.9 ± 241.4 $mm^3$ at day 54 after injection. In contrast, tumor volumes in mice with *BRCA1P1*-KO cells ($n = 9$) remained below 50 $mm^3$ for all mice throughout the study. Tumors for this group of mice were below measurable limits after day 30, except for one mouse with a tumor that reached 42 $mm^3$ by day 54 (**Fig. 6A**). Because our *in vitro* studies showed increased cytokine expression in *BRCA1P1*-depleted cells compared with WT cells (**Fig. 2D** and **E**), we also assessed immune responses regulated by *BRCA1P1* in our xenograft mouse model. Because athymic nude mice lack T cells, we measured cytokine expression in spleen tissues harvested from mice with *BRCA1P1*-WT and *BRCA1P1*-KO tumors. The transcript amounts of the cytokines TNFα, IL2, IFNγ, and IL12a in the spleen were significantly higher in mice with *BRCA1P1*-KO tumors compared with control mice with WT tumors (**Fig. 6B**). Collectively, these data suggest that *BRCA1P1* depletion suppresses tumor growth partly through stimulation of local immunity, ultimately leading to reduced proliferation and enhanced apoptosis of cancer cells.

## Discussion

Innate immune defense pathways are critical for antitumor responses and the induction of apoptosis of cancer cells (1). Although the importance of antiviral mechanism is well known in cancer, the roles of host RNAs in antiviral defense mechanism have just begun to be elucidated. In this study, we discovered an immunogenic role for *BRCA1P1*-lncRNA in regulating antiviral defense mechanisms in breast cancer cells. Spread of a viral infection is restricted by three major defense mechanisms (22). The first involves the upregulation and activation of a set of antiviral proteins, which allow for virus sensing and attenuation of virus replication. The second, more drastic mechanism is the apoptosis of infected cells. The third is based on paracrine IFN signaling, which alerts noninfected cells. *BRCA1P1* is potentially involved in all three mechanisms. *BRCA1P1*-deficient cells were prone to apoptosis and highly expressed antiviral immune genes, including IFNs, which are typical markers of virus-infected cells. Depletion of *BRCA1P1* suppressed tumor growth and stimulated local immunity in a breast cancer xenograft mouse model. Our findings thus reveal a novel mechanism of regulation of antiviral responses by a host pseudogene RNA in breast cancer cells.

Mechanistically, *BRCA1P1*-lncRNA binds the NF-κB subunit RelA, inhibits the activity of RelA at its target promoters, and thereby negatively regulates transcription of antiviral genes. It is of note that *BRCA1P1*-lncRNA appears to interact with RelA irrespective of whether RelA dissociates (**Fig. 4E–G**) or associates with chromatin (**Fig. 4B**; Supplementary Fig. S7B). It has been reported that the NF-κB complex binds chromatin and recruits a chromatin-modifying complex (28–30). Specifically, the RelA subunit of NF-κB was reported to interact with histone deacetylases on chromatin (30). Thus, when *BRCA1P1*-lncRNA associates with RelA, it is likely to interact with histones indirectly through chromatin-bound RelA. In support of this, the level of *BRCA1P1* enrichment on H2B (0.59 ± 0.02, relative unit) or H3 (0.47 ± 0.03) is similar to that of RelA (0.54 ± 0.08; **Fig. 4B**; Supplementary Fig. S7B). Considering the vast numbers of nucleosome-associated histones on every chromosome, the data indicate that only a very small portion of histones associates with *BRCA1P1*-lncRNA, likely through RelA bound on chromatin. Although further investigation will be required to determine the detailed mechanisms of *BRCA1P1*-regulated RelA activity, our data revealed a strong association of *BRCA1P1*-lncRNA with RelA. Interestingly, recent discoveries showed that cellular noncoding transcripts bind to RIG-I and/or its activator, the E3 ligase TRIM25, and promote RIG-I–mediated antiviral innate immune responses (8, 31, 32). Therefore, it is conceivable that there may be additional mechanisms through which *BRCA1P1* activates antiviral signaling, such as a direct effect of *BRCA1P1*-lncRNA on immunostimulatory dsRNAs or their sensors, or by regulating the activity of dsRNA-activated kinases, which warrants future investigation.

Our data also showed that *BRCA1P1* depletion stimulates the induction of proinflammatory cytokines in the spleen of our mouse

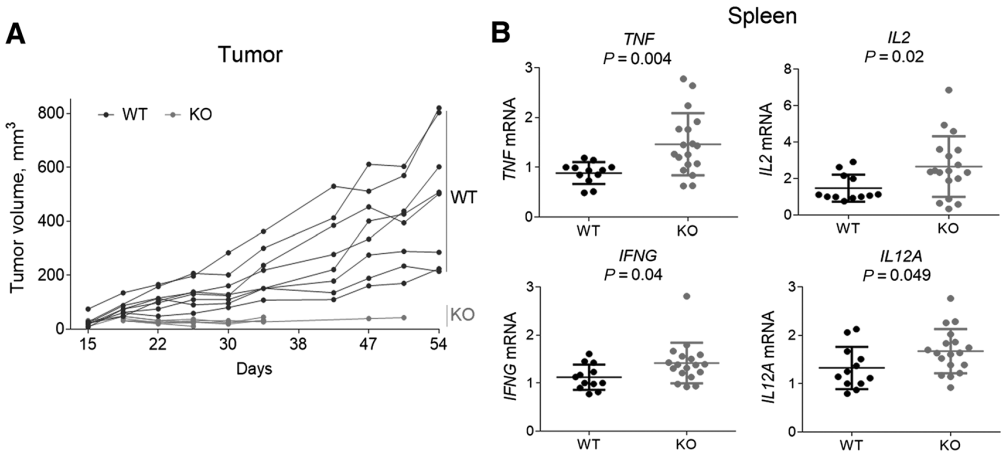


**Figure 6.**

Tumor volume and cytokine expression in a *BRCA1P1*-KO xenograft mouse model. **A,** Tumor measurements were performed weekly starting at day 15 after cell injection. Each line represents the average weekly tumor volume in an animal during the study. **B,** Expression of proinflammatory cytokines (*TNF, IL2, IFNG*, and *IL12A* mRNAs) was measured by qRT-PCR in spleen tissues collected at the end of the study. The data showed that the transcript amounts of the proinflammatory cytokines in the spleen were significantly higher in mice with *BRCA1P1*-KO tumors compared with control mice with WT tumors ($P < 0.05$). Fold change is shown relative to control mice with WT tumors. Two independent qRT-PCR experiments were performed and each dot represents the mean of $n = 4$ biological replicates.

Published OnlineFirst January 20, 2021; DOI: 10.1158/0008-5472.CAN-20-1959



model, suggesting an important role for *BRCA1P1* in regulating local immunity. However, because athymic nude mice lack T cells, we were unable to evaluate the effects of *BRCA1P1*-deficiency on T cells or other immune cells. Therefore, future studies using humanized mice will be needed to fully understand the role of *BRCA1P1*-lncRNA in modulating local immunity and the tumor microenvironment. Along these lines, as NF-κB plays multiple roles in innate immunity and pro-inflammatory signaling, further investigation will be required to examine how NF-κB regulates *BRCA1P1* depletion-driven antiviral immunity in a context-dependent manner. It also remains to be determined whether the interaction of *BRCA1P1*-lncRNA with RelA influences the RelA-mediated transcription of apoptosis genes, which may contribute to increased apoptosis in *BRCA1P1*-KO cells. In addition, future studies on the detailed mechanisms of how *BRCA1P1* expression is regulated by upstream signals may increase our understanding of the regulatory circuits in *BRCA1P1*-mediated responses.

Despite some limitations, our study revealed a novel mechanism of innate immunity that is regulated by a pseudogene lncRNA. Regulation of innate immunity by the *BRCA1P1* pseudogene might open up new possibilities for multilayered immunotherapy for cancer control (33). Tumor immunity and immunotherapy have become increasingly important in treatment strategies for a variety of tumors. They also point to etiology and progression pathways that could be targeted for prevention. Clinical trials evaluating the safety and efficacy of intratumoral injection of STING agonists, TLR agonists, or poly(I:C) derivatives with innate immune modulators are currently completed or are ongoing (34–37). Oncolytic viruses have also emerged as important agents in cancer treatment as they offer the attractive therapeutic combination of tumor-specific cell lysis together with immune stimulation (33, 38). Considering the importance of innate immunity and antiviral sensing in tumor immunity, our findings on the regulation of innate immunity by *BRCA1P1* may have clinical relevance in the development of immunotherapies and should be further explored.

## Authors' Disclosures

J. Zhang reports grants from NCI P20CA233307, as well as other funding from Breast Cancer Research Foundation, Kiphart Global Health Research Fund, and grants from NIH R01 AI087846 during the conduct of the study. O. Karginova reports grants from Breast Cancer Research Foundation during the conduct of the study. Q. Hao reports grants from University of Illinois at Urbana-Champaign during the conduct of the study. A. Prat reports personal fees from Nanostring Technologies, Astrazeneca, Roche, Novartis, Foundation Medicine, BMS, Daiichi Sankyo, Oncolytics Biotech, and Guardant Health outside the submitted work. K.V. Prasanth reports grants from NIA/NIH, NSF/EAGER, and NIGMS/NIH during the conduct of the study. O.I. Olopade reports other funding from CancerIQ, Tempus, and 54gene outside the submitted work. No other disclosures were reported.

## Authors' Contributions

**Y.J. Han:** Conceptualization, data curation, formal analysis, supervision, funding acquisition, validation, investigation, visualization, methodology, writing–original draft, project administration. **J. Zhang:** Formal analysis, validation, investigation, methodology, writing–review and editing. **J.-H. Lee:** Formal analysis, investigation, visualization, methodology. **J.M. Mason:** Formal analysis, investigation, visualization, methodology, writing–review and editing. **O. Karginova:** Formal analysis, investigation, visualization, writing–review and editing. **T.F. Yoshimatsu:** Formal analysis, investigation, methodology, writing–review and editing. **Q. Hao:** Formal analysis, investigation, visualization, methodology. **I. Hurley:** Investigation, methodology, writing–review and editing. **L.P. Brunet:** Formal analysis, investigation. **A. Prat:** Formal analysis, investigation. **K.V. Prasanth:** Formal analysis, funding acquisition, investigation, methodology, writing–review and editing. **M.U. Gack:** Conceptualization, data curation, formal analysis, supervision, funding acquisition, investigation, methodology, writing–review and editing. **O.I. Olopade:** Conceptualization, resources, data curation, supervision, funding acquisition, investigation, project administration, writing–review and editing.

## Acknowledgments

We thank Drs. Fengyi Wan and Yifan Lei at the Department of Biochemistry and Molecular Biology, Johns Hopkins University, for their generous providing of truncated mutant constructs of RelA. We appreciate Lise Sveen's careful review on the article. We also thank Mariann Coyle and Maria Gomez-Vega for their assistance with cell culturing and fluorescence *in situ* hybridization. This work was supported by NCI P20CA233307 (to O.I. Olopade), Breast Cancer Research Foundation BCRF-20-071 (to O.I. Olopade and Y.J. Han), and the Kiphart Global Health Research Fund (to O.I. Olopade). This study was further supported in part by NIH R01 AI087846 (to M.U. Gack). The K.V. Prasanth laboratory is funded by grants from Cancer Center at Illinois seed grant and Prairie Dragon Paddlers, NIH R21AG065748, NIH R01GM132458, and NSF EAGER grant (MCB1723008). O.I. Olopade is an American Cancer Society Clinical Research Professor.

The costs of publication of this article were defrayed in part by the payment of page charges. This article must therefore be hereby marked *advertisement* in accordance with 18 U.S.C. Section 1734 solely to indicate this fact.

Received June 9, 2020; revised October 28, 2020; accepted January 13, 2021; published first January 20, 2021.

## References

1. Minn AJ. Interferons and the immunogenic effects of cancer therapy. Trends Immunol 2015;36:725–37.
2. Wies E, Wang MK, Maharaj NP, Chen K, Zhou S, Finberg RW, et al. Dephosphorylation of the RNA sensors RIG-I and MDA5 by the phosphatase PP1 is essential for innate immune signaling. Immunity 2013;38:437–49.
3. Rehwinkel J, Gack MU. RIG-I–like receptors: their regulation and roles in RNA sensing. Nat Rev Immunol 2020;20:537–51.
4. Schoggins JW, Rice CM. Interferon-stimulated genes and their antiviral effector functions. Curr Opin Virol 2011;1:519–25.
5. Sistigu A, Yamazaki T, Vacchelli E, Chaba K, Enot DP, Adam J, et al. Cancer cell-autonomous contribution of type I interferon signaling to the efficacy of chemotherapy. Nat Med 2014;20:1301–9.
6. Balakirev ES, Ayala FJ. Pseudogenes: are they "junk" or functional DNA? Annu Rev Genet 2003;37:123–51.
7. Zhang Z, Harrison PM, Liu Y, Gerstein M. Millions of years of evolution preserved: a comprehensive catalog of the processed pseudogenes in the human genome. Genome Res 2003;13:2541–58.
8. Chiang JJ, Sparrer KMJ, van Gent M, Lassig C, Huang T, Osterrieder N, et al. Viral unmasking of cellular 5S rRNA pseudogene transcripts induces RIG-I–mediated immunity. Nat Immunol 2018;19:53–62.
9. Rapicavoli NA, Qu K, Zhang J, Mikhail M, Laberge RM, Chang HY. A mammalian pseudogene lncRNA at the interface of inflammation and anti-inflammatory therapeutics. Elife 2013;2:e00762.
10. Barker DF, Liu X, Almeida ER. The BRCA1 and 1A1.3B promoters are parallel elements of a genomic duplication at 17q21. Genomics 1996;38:215–22.
11. Brown MA, Xu CF, Nicolai H, Griffiths B, Chambers JA, Black D, et al. The 5′ end of the BRCA1 gene lies within a duplicated region of human chromosome 17q21. Oncogene 1996;12:2507–13.
12. Pettigrew CA, French JD, Saunus JM, Edwards SL, Sauer AV, Smart CE, et al. Identification and functional analysis of novel BRCA1 transcripts, including mouse Brca1-Iris and human pseudo-BRCA1. Breast Cancer Res Treat 2010;119:239–47.
13. Puget N, Gad S, Perrin-Vidoz L, Sinilnikova OM, Stoppa-Lyonnet D, Lenoir GM, et al. Distinct BRCA1 rearrangements involving the BRCA1

pseudogene suggest the existence of a recombination hot spot. Am J Hum Genet 2002;70:858–65.
14. Khanna KK, Jackson SP. DNA double-strand breaks: signaling, repair and the cancer connection. Nat Genet 2001;27:247–54.
15. Scully R, Ganesan S, Vlasakova K, Chen J, Socolovsky M, Livingston DM. Genetic analysis of BRCA1 function in a defined tumor cell line. Mol Cell 1999;4:1093–9.
16. Miki Y, Swensen J, Shattuck-Eidens D, Futreal PA, Harshman K, Tavtigian S, et al. A strong candidate for the breast and ovarian cancer susceptibility gene BRCA1. Science 1994;266:66–71.
17. Han YJ, Boatman SM, Zhang J, Du XC, Yeh AC, Zheng Y, et al. LncRNA BLAT1 is upregulated in basal-like breast cancer through epigenetic modifications. Scientific Reports 2018;8:15572.
18. Ran FA, Hsu PD, Wright J, Agarwala V, Scott DA, Zhang F. Genome engineering using the CRISPR-Cas9 system. Nat Protoc 2013;8:2281–308.
19. Parker JS, Mullins M, Cheang MC, Leung S, Voduc D, Vickery T, et al. Supervised risk predictor of breast cancer based on intrinsic subtypes. J Clin Oncol 2009;27: 1160–7.
20. Kato H, Sato S, Yoneyama M, Yamamoto M, Uematsu S, Matsui K, et al. Cell type-specific involvement of RIG-I in antiviral response. Immunity 2005;23: 19–28.
21. Reikine S, Nguyen JB, Modis Y. Pattern recognition and signaling mechanisms of RIG-I and MDA5. Front Immunol 2014;5:342.
22. Czerkies M, Korwek Z, Prus W, Kochanczyk M, Jaruszewicz-Blonska J, Tudelska K, et al. Cell fate in antiviral response arises in the crosstalk of IRF, NF-kappa B and JAK/STAT pathways. Nat Commun 2018;9:493.
23. Wajant H, Pfizenmaier K, Scheurich P. Tumor necrosis factor signaling. Cell Death Differ 2003;10:45–65.
24. Voltan R, Secchiero P, Casciano F, Milani D, Zauli G, Tisato V. Redox signaling and oxidative stress: cross talk with TNF-related apoptosis inducing ligand activity. Int J Biochem Cell Biol 2016;81:364–74.
25. Kamata H, Honda S, Maeda S, Chang L, Hirata H, Karin M. Reactive oxygen species promote TNF alpha-induced death and sustained JNK activation by inhibiting MAP kinase phosphatases. Cell 2005;120:649–61.
26. Wheelhouse NM, Chan YS, Gillies SE, Caldwell H, Ross JA, Harrison DJ, et al. TNF-alpha induced DNA damage in primary murine hepatocytes. Int J Mol Med 2003;12:889–94.
27. Yan B, Wang H, Rabbani ZN, Zhao Y, Li W, Yuan Y, et al. Tumor necrosis factor-alpha is a potent endogenous mutagen that promotes cellular transformation. Cancer Res 2006;66:11565–70.
28. Bhatt D, Ghosh S. Regulation of the NF-kappa B-mediated transcription of inflammatory genes. Front Immunol 2014;5:71.
29. Lone IN, Shukla MS, Charles Richard JL, Peshev ZY, Dimitrov S, Angelov D. Binding of NF-kappaB to nucleosomes: effect of translational positioning, nucleosome remodeling and linker histone H1. PLoS Genet 2013; 9:e1003830.
30. Ashburner BP, Westerheide SD, Baldwin AS Jr. The p65 (RelA) subunit of NF-kappa B interacts with the histone deacetylase (HDAC) corepressors HDAC1 and HDAC2 to negatively regulate gene expression. Mol Cell Biol 2001;21:7065–77.
31. Lin H, Jiang M, Liu L, Yang Z, Ma Z, Liu S, et al. The long noncoding RNA Lnczc3h7a promotes a TRIM25-mediated RIG-I antiviral innate immune response. Nat Immunol 2019;20:812–23.
32. Jiang M, Zhang S, Yang Z, Lin H, Zhu J, Liu L, et al. Self-recognition of an inducible host lncRNA by RIG-I feedback restricts innate immune response. Cell 2018;173:906–19.
33. Demaria O, Cornen S, Daeron M, Morel Y, Medzhitov R, Vivier E. Harnessing innate immunity in cancer therapy. Nature 2019;574:45–56.
34. Brody JD, Ai WZ, Czerwinski DK, Torchia JA, Levy M, Advani RH, et al. *In situ* vaccination with a TLR9 agonist induces systemic lymphoma regression: a phase I/II study. J Clin Oncol 2010;28:4324–32.
35. Demaria O, De Gassart A, Coso S, Gestermann N, Di Domizio J, Flatz L, et al. STING activation of tumor endothelial cells initiates spontaneous and therapeutic antitumor immunity. Proc Natl Acad Sci U S A 2015;112: 15408–13.
36. Dowling DJ, Tan Z, Prokopowicz ZM, Palmer CD, Matthews MA, Dietsch GN, et al. The ultra-potent and selective TLR8 agonist VTX-294 activates human newborn and adult leukocytes. PLoS ONE 2013;8:e58164.
37. Caskey M, Lefebvre F, Filali-Mouhim A, Cameron MJ, Goulet JP, Haddad EK, et al. Synthetic double-stranded RNA induces innate immune responses similar to a live viral vaccine in humans. J Exp Med 2011;208:2357–66.
38. Gujar S, Pol JG, Kim Y, Lee PW, Kroemer G. Antitumor benefits of antiviral immunity: an underappreciated aspect of oncolytic virotherapies. Trends Immunol 2018;39:209–21.

Published OnlineFirst January 20, 2021; DOI: 10.1158/0008-5472.CAN-20-1959

AACR American Association for Cancer Research

Cancer Research
The Journal of Cancer Research (1916–1930) | The American Journal of Cancer (1931–1940)

# The *BRCA1* Pseudogene Negatively Regulates Antitumor Responses through Inhibition of Innate Immune Defense Mechanisms

Yoo Jane Han, Jing Zhang, Jung-Hyun Lee, et al.

*Cancer Res* 2021;81:1540-1551. Published OnlineFirst January 20, 2021.